ACS central science

Research Article

Cite This: ACS Cent. Sci. 2019, 5, 477−485

http://pubs.acs.org/journal/acscii

Promoting Angiogenesis in Oxidative Diabetic Wound Microenvironment Using a Nanozyme-Reinforced Self-Protecting Hydrogel

Haibin Wu,[†,⊥] Fangyuan Li,[†,‡,⊥] Wei Shao,[†] Jianqing Gao,[*,†,§] and Daishun Ling[*,†,‡,∥]

[†]Institute of Pharmaceutics, College of Pharmaceutical Sciences, Zhejiang University, Hangzhou 310058, P. R. China

[‡]Hangzhou Institute of Innovative Medicine, College of Pharmaceutical Sciences, Zhejiang University, Hangzhou 310012, P. R. China

[§]Dr. Li Dak Sum & Yip Yio Chin Center for Stem Cell and Regenerative Medicine, Zhejiang University, Hangzhou 310058, P. R. China

[∥]Key Laboratory of Biomedical Engineering of the Ministry of Education, College of Biomedical Engineering & Instrument Science, Zhejiang University, Hangzhou 310027, P. R. China

Supporting Information

ABSTRACT: Impaired diabetic wound healing represents a devastating and rapidly growing clinical problem associated with high morbidity, mortality, and recurrence rates. Engineering therapeutic angiogenesis in the wounded tissue is critical for successful wound healing. However, stimulating functional angiogenesis of the diabetic wound remains a great challenge, due to the oxidative damage and denaturation of bio-macromolecule-based angiogenic agents in the oxidative diabetic wound microenvironment. Here, we present a unique "seed-and-soil" strategy that circumvents the limitation by simultaneously reshaping the oxidative wound microenvironment into a proregenerative one (the "soil") and providing proangiogenic miRNA cues (the "seed") using an miRNA-impregnated, redox-modulatory ceria nanozyme-reinforced self-protecting hydrogel (PCN-miR/Col). The PCN-miR/Col not only reshapes the hostile oxidative wound microenvironment, but also ensures the structural integrity of the encapsulated proangiogenic miRNA in the oxidative microenvironment. Diabetic wounds treated with the PCN-miR/Col demonstrate a remarkably accelerated wound closure and enhanced quality of the healed wound as featured by highly ordered alignment of collagen fiber, skin appendage morphogenesis, functional new blood vessel growth, and oxygen saturation.

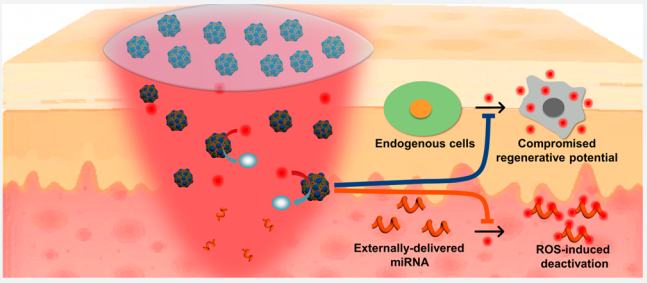

INTRODUCTION

Impaired diabetic wound healing is the most common complication in patients with diabetic hyperglycemia, which suffers from high morbidity, mortality, and recurrence rates and is the leading cause of nontraumatic limb amputations worldwide.[1,2] Increasing evidence suggests that defective angiogenesis significantly contributes to the debilitating conditions in impaired diabetic wound healing, which limits the delivery of crucial oxygen and nutrient to the wounded tissue thus impairing the wound healing process.[1,3,4] Furthermore, excessive oxidative stress also plays a critical role in the pathology of impaired diabetic wound healing.[5] Under this hostile wound microenvironment, the uncontrolled accumulation of reactive oxygen species (ROS) leads to significant destruction of endogenous stem cells, growth factors, and nucleic acids in the wounded tissue and thus greatly compromises their regenerative potential.[4,6−8] In addition, the externally administered proteins and nucleic acids are also highly vulnerable in the harsh diabetic wound microenvironment.[6,9] Moreover, it is noteworthy that these two pathological factors, defective angiogenesis and excessive oxidative stress, are not independent of each other since excessive ROS has been proposed to restrict angiogenic responses and result in endothelial dysfunction.[10,11] Current clinical therapies including debridement, antibiotics, blood-glucose control, and living skin-equivalent grafts mainly focus on preventing the expansion of the initial wound bed and infection.[12] Although symptom control maybe achieved by these standard therapies, therapeutics for effectively regeneration of the diabetic wound remains elusive. Unfortunately, ∼10% of diabetic wound patients will eventually undergo limb amputation.[12,13]

Among various efforts to address this urgent issue, reconstruction of functional vascularity is of vital importance.[3,14] Despite significant advances being made in improving angiogenesis in diabetic wounds by supplementing either angiogenic cells or growth factors, the achievements

Received: November 18, 2018
Published: February 13, 2019

DOI: 10.1021/acscentsci.8b00850
ACS Cent. Sci. 2019, 5, 477−485

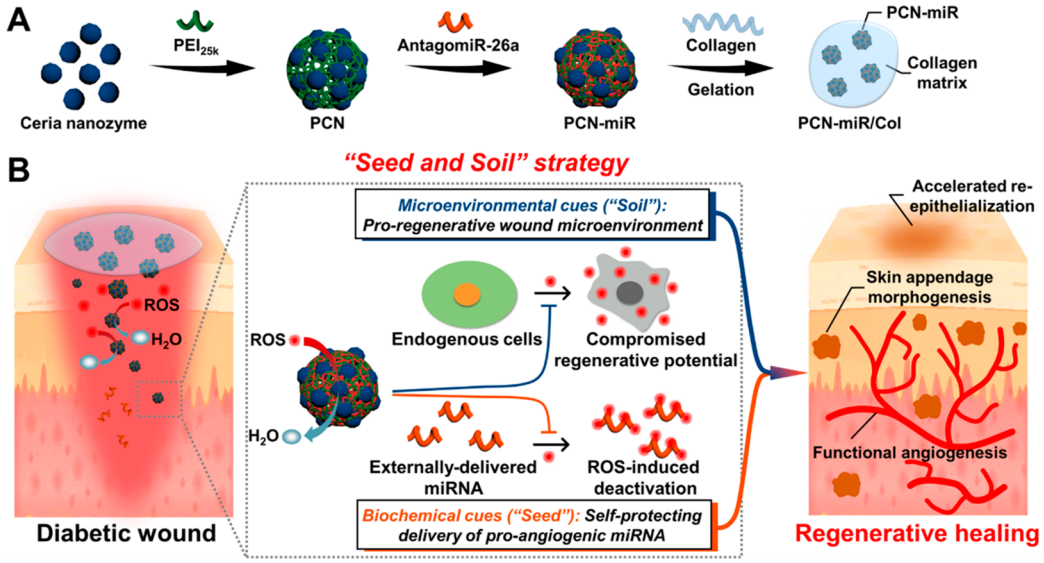

Figure 1. Schematic illustration of the fabrication process for the PCN-miR/Col hydrogel, and the strategy for functional angiogenesis and regenerative diabetic wound healing. (A) Schematic illustration of the fabrication routes for PCN-miR/Col. (B) Schematic illustration of the PCN-miR/Col-enabled strategy for simultaneous self-protecting delivery of proangiogenic miRNA cues and creation of proregenerative wound microenvironment to drive highly efficient functional angiogenesis and regenerative diabetic wound healing.

made so far have failed to translate into a meaningful clinical improvement because of a number of drawbacks.[15,16] A promising alternative to cells or growth factors for efficient angiogenesis is miRNA,[17] a class of highly conserved small noncoding regulatory RNAs, since accumulating evidence has demonstrated that miRNAs are involved in the development of defective angiogenesis.[18] Specifically, miR-26a has been recently identified as a key negative regulator of angiogenesis in diabetic wounds; inhibition of this miRNA may serve as a promising therapeutic modality.[18] Remarkably, targeting the disease-associated miRNA is a potentially more potent therapeutic strategy in comparison with single-target angiogenic growth factors since an individual miRNA with its pleiotropic effects can regulate multiple different genes and processes.

Although various nonviral or viral vectors have been explored for delivering these promising miRNAs in inhibition and replacement therapies,[19,20] an insurmountable obstacle is their rapid breakdown and inactivation in the hostile disease microenvironment,[9] which in the case of the diabetic wound, is the excessive oxidative stress.[6] Nevertheless, in addition to the diabetic wound, excessive ROS are also tightly linked with a myriad of serious diseases, where miRNAs could serve as promising therapeutic approaches.[21] Unfortunately, to the best of our knowledge, studies devoted to the design and construction of highly efficient miRNA carriers with a self-protecting capacity in the hostile oxidative disease microenvironment have been rarely reported so far. Meanwhile, engineering a friendly wound microenvironment is increasingly recognized as a novel paradigm for the successful healing of diabetic wound.[5,6] Accordingly, materials designed to simultaneously deliver proangiogenic miRNA cues (the "seed") in a self-protecting manner and reshape the hostile oxidative wound microenvironment (the "soil") are therefore highly desired yet challenging for functional angiogenesis and regenerative diabetic wound healing.

Recent advances in nanotechnology for biomedical applications have enabled elegant solutions for these problems.[22] As a representative nanozyme, ceria nanocrystals have recently drawn great attention in the treatment of oxidative-stress-associated diseases due to their facile synthesis, excellent biocompatibility, superior multiple antioxidant enzyme-mimetic activity, and rejuvenated catalytic performance.[23,24] These beneficial intrinsic properties of ceria nanozyme make it superior to other conventional antioxidant molecules or enzymes since they usually suffer from respective and collective drawbacks such as poor stability, high cost, scavenging only a single type of ROS, and nonrenewable ROS-scavenging capacity.[25] Furthermore, in comparison with the systemic administration route, we hypothesize that topical miRNA delivery by an miRNA-containing hydrogel depot may be favorable for their therapeutic effects in a site-specific manner, without raising concerns about systemic toxicity and off-target side effects.[26−28] On the basis of these considerations, herein we introduce a unique "seed-and-soil" strategy for enhanced diabetic wound healing using a nanozyme-reinforced self-protecting hydrogel (PCN-miR/Col) composed of 25 kDa polyethylenimine (PEI_{25K}) functionalized ceria nanocluster (PCN) antagomiR-26a (miR) nanocomplex (PCN-miR), which is designed to simultaneously reshape the hostile wound microenvironment (the "soil") and provide proangiogenic cues (the "seed") for diabetic wound repair and regeneration (Figure 1A,B). The natural extracellular matrix protein collagen was employed for the construction of the hydrogel, which serves as a favorable platform for the integration of the PCN-miR. AntagomiR-26a was utilized to inhibit the antiangiogenic miR-26a, a well-established hyperglycemia-induced target that is responsible for impaired angiogenesis in diabetic wounds.[18] Benefited from the highly efficient ROS-scavenging activities, PCN-miR/Col not only enable reformation of the hostile oxidative wound microenvironment, but also protect the encapsulated miRNAs against ROS-induced damage. Because of the extraordinary synergy, augmented functional blood vessel growth and oxygen saturation were achieved, resulting in an accelerated wound closure and a superior quality of the newly healed wound

DOI: 10.1021/acscentsci.8b00850
ACS Cent. Sci. 2019, 5, 477−485

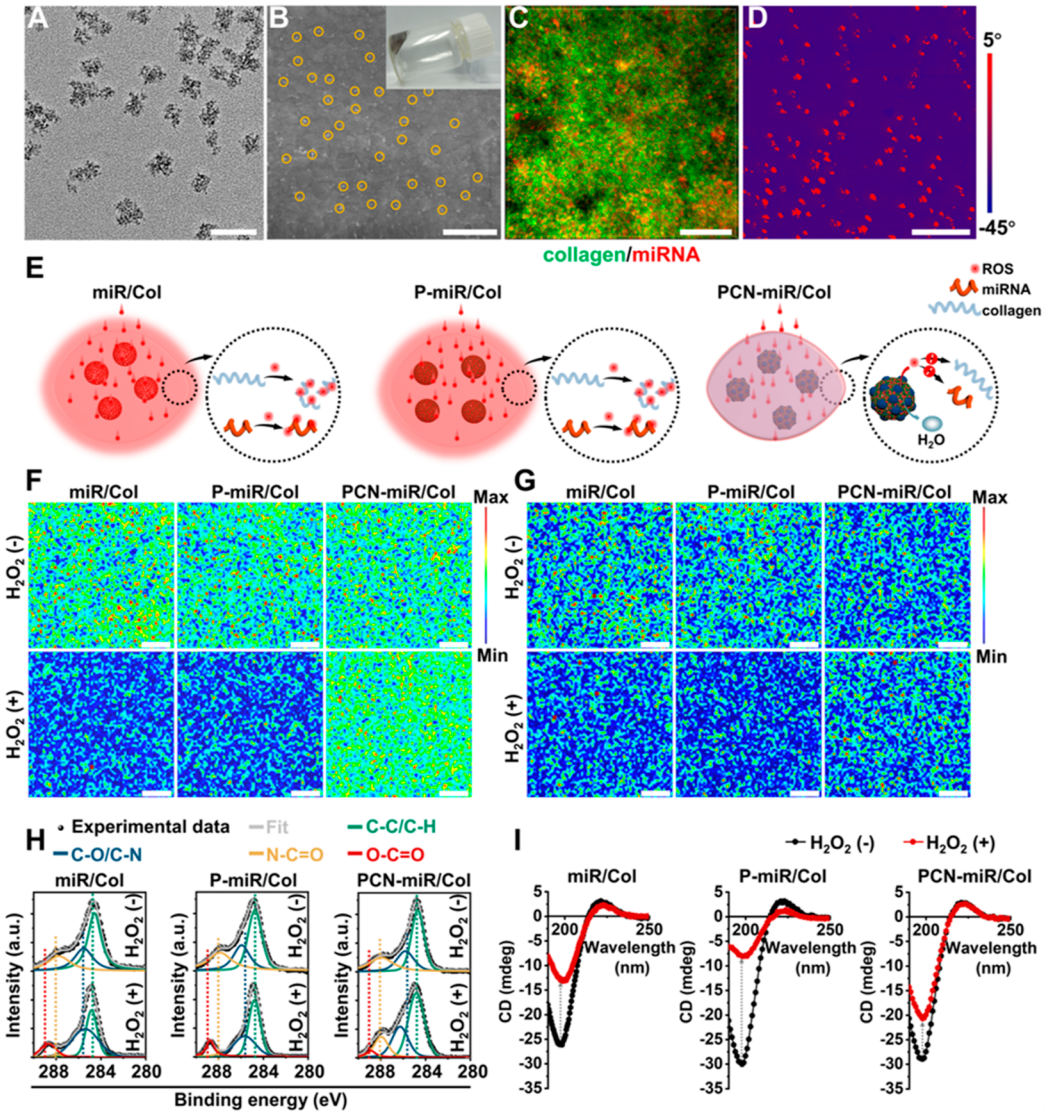

Figure 2. Characterization of PCN-miR/Col hydrogel and their resistance to oxidative denaturation. (A) TEM image of PCN-miR. Scale bar, 50 nm. (B) SEM image of the surface of PCN-miR/Col (inset: digital photograph of PCN-miR/Col hydrogel). The PCN-miR (marked by yellow solid circles) was clearly observed. Scale bar, 1 μm. (C) Three-dimensional confocal laser scanning microscopy (CLSM) image of PCN-miR/Col, where collagen from the hydrogel is labeled with fluorescein isothiocyanate (green), and antagomiR-26a is tagged with Cy5 (red). Scale bar, 100 μm. (D) AFM phase image of PCN-miR/Col. Scale bar, 500 nm. (E) Schematic illustration of the responses of collagen-based hydrogels under ROS exposure. Confocal Raman mapping of collagen-based hydrogels before (upper panel) and after (lower panel) exposure to H_2O_2: (F) the 1280 cm^{-1} peak corresponds to the amide III from collagen, and (G) the 810 cm^{-1} peak corresponds to the backbone O-P-O stretching from antagomiR-26a. Scale bars, 20 μm. (H) Deconvoluted high-resolution C1s XPS and (I) CD spectra of collagen-based hydrogels with or without exposure to H_2O_2. The XPS spectra were fitted to four energy components centered at around 284.6 (C-C/C-H), 285.5 (C-O/C-N), 287.8 (N-C═O), and 288.6 (O-C═O) eV.

featured by ordered alignment of collagen fiber and skin appendage morphogenesis. The proposed "seed-and-soil" strategy is applicable to the repair and regeneration of a broad range of damaged tissues, which suffer from highly oxidative diseased microenvironments and dysregulated biomacromolecules.

RESULTS AND DISCUSSION

Fabrication of PCN-miR/Col Hydrogel and Resistance to Oxidative Denaturation. The facile process to fabricate PCNs begins with the synthesis of ultrasmall (~3 nm in diameter) ceria nanozymes (Figure S1A),[23] followed by surface modification with PEI_{25K}. The PCN-miR was subsequently prepared by electrostatic interaction between negatively charged antagomiR-26a and positively charged PCNs. The intimate contact of ceria nanozyme and miRNA enabled by covalent modification of ceria nanozyme with PEI_{25K} allows an all-weather protection of impregnated miRNA against oxidative damage, which is advantageous over simple combination or sequential delivery of ceria nanozyme and PEI_{25k}-miRNA complex. As shown in the transmission electron microscopy (TEM) image, the prepared PCN-miR has a size of ~20 nm (Figure 2A, Figure S1B,C). An increased N:P ratio led to a smaller size and more positive charge of PCN-miR, as revealed by dynamic light scattering (DLS) and ζ-potential measurements (Figure S1D,E). The agarose gel retardation assay indicates that antagomiR-26a binds to PCNs with a N:P ratio (the ratio of nitrogen in PEI_{25K} to the phosphorus in

DOI: 10.1021/acscentsci.8b00850
ACS Cent. Sci. 2019, 5, 477−485

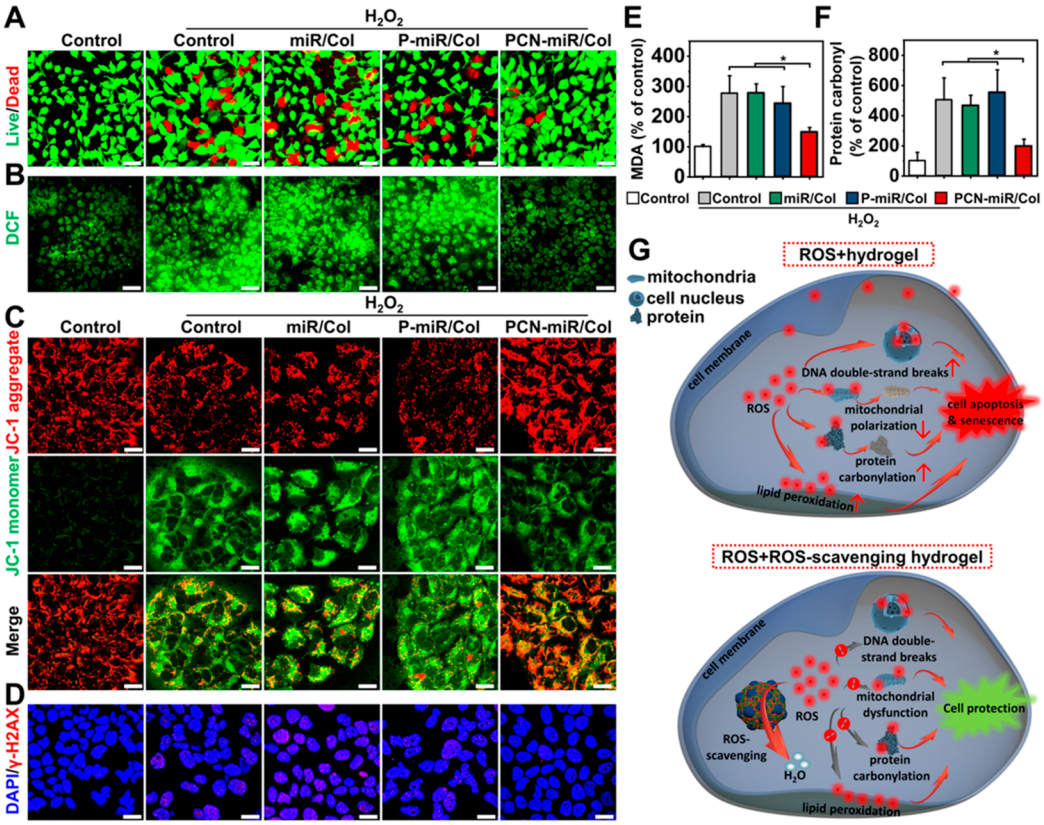

Figure 3. Incubation with the PCN-miR/Col confers robust protection to ROS-exposed cells. (A) Pretreatment of HUVECs with PCN-miR/Col abrogated H_2O_2-induced cell viability loss as indicated by live/dead staining with calcein-AM (green) and propidium iodide (red). Scale bars, 50 μm. (B) Representative CLSM images showing the H_2O_2-induced intracellular ROS accumulation in HUVECs with various pretreatments, using DCF-DA as an ROS indicator. Scale bars, 50 μm. Representative confocal images of (C) JC-1 (a mitochondrial membrane potential-sensitive probe) and (D) γ-H2AX (a marker of DNA double-strand breaks) staining in cells with various pretreatments after exposure to H_2O_2. Scale bars, 20 μm. (E) Lipid peroxidation product MDA and (F) protein carbonylation levels in cells with various pretreatments after exposure to H_2O_2. All results are presented as mean ± SD, $^*P < 0.05$ by two-tailed unpaired Student's t tests, $n = 3$. (G) Schematic illustration of the ROS-induced damage responses in cells cultured on collagen-based hydrogels.

antagomiR-26a) >5 (Figure S1F). Notably, there is no significant change in the DLS size and ζ-potential of PCN-miR when the N:P ratio is greater than 10, whereas severe cytotoxicity could be induced at higher N:P ratios.[29] Therefore, a N:P ratio of 10 was chosen for the further experiments.

The gelation kinetics of the PCN-miR/Col were monitored (Figure S2A).[30] From the scanning electron microscopy (SEM) images, the surfaces of naked antagomiR-26a-loaded (miR-loaded) collagen hydrogel (miR/Col) and PEI_{25k} (P) antagomiR-26a (miR) complex-doped collagen hydrogel (P-miR/Col) are clean and smooth, while the surface of PCN-miR/Col is homogeneously doped with PCN-miR (Figure 2B, Figure S2B). Furthermore, energy-dispersive X-ray (EDX) elemental mapping results clearly indicate the uniform existence of C, N, S, and Ce elements in PCN-miR/Col (Figure S2C). Fluorescently labeled antagomiR-26a within the P-miR/Col and PCN-miR/Col demonstrates a good distribution uniformity due to the electrostatic repulsion elicited by the PEI_{25K} polycations, whereas an evident aggregation was observed in the matrix of the miR/Col (Figure 2C, Figure S2D). Compared to the soft property of the polymer in miR/Col and P-miR/Col, the metallic ceria nanozymes in the PCN-miR/Col exhibited the stiffness as demonstrated by the atomic force microscopy (AFM) phase images (Figure 2D, Figure S2E).

Recent studies indicate that hydrogen peroxide (H_2O_2) is overproduced in diabetic complications and can convert to various highly reactive radicals;[31,32] therefore, we employed H_2O_2 to simulate the oxidative stress microenvironment. The influence of H_2O_2 exposure on the structural and conformational integrity of the incorporated antagomiR-26a and collagen matrix was further investigated (Figure 2E). A significant decrease in Raman signals for collagen and antagomiR-26a was detected after exposure of miR/Col and P-miR/Col to ROS, whereas only a slight change of the Raman signals was detected on the ceria nanozyme-doped PCN-miR/Col (Figure 2F,G). These changes in Raman features clearly indicated the denaturation of the collagen matrix and antagomiR-26a in miR/Col and P-miR/Col, whereas the structural integrity of these bioactive macromolecules was largely preserved in PCN-miR/Col, suggesting that incorporated ROS-scavenging ceria nanozymes could mitigate the consequences of oxidative damage.[23,33] This is a highly desired property for application of bio-macromolecule-based therapeutics, since proteins and nucleic acids are generally prone to denature in highly oxidative conditions.[34]

In accordance with the Raman mapping results, the deconvoluted high-resolution C1s X-ray photoelectron spectra (XPS) displayed an obvious new peak at around 288.6 eV corresponding to the O-C═O bond, while the peak corresponding to the N-C═O bond (287.8 eV) decreased

DOI: 10.1021/acscentsci.8b00850
ACS Cent. Sci. 2019, 5, 477−485

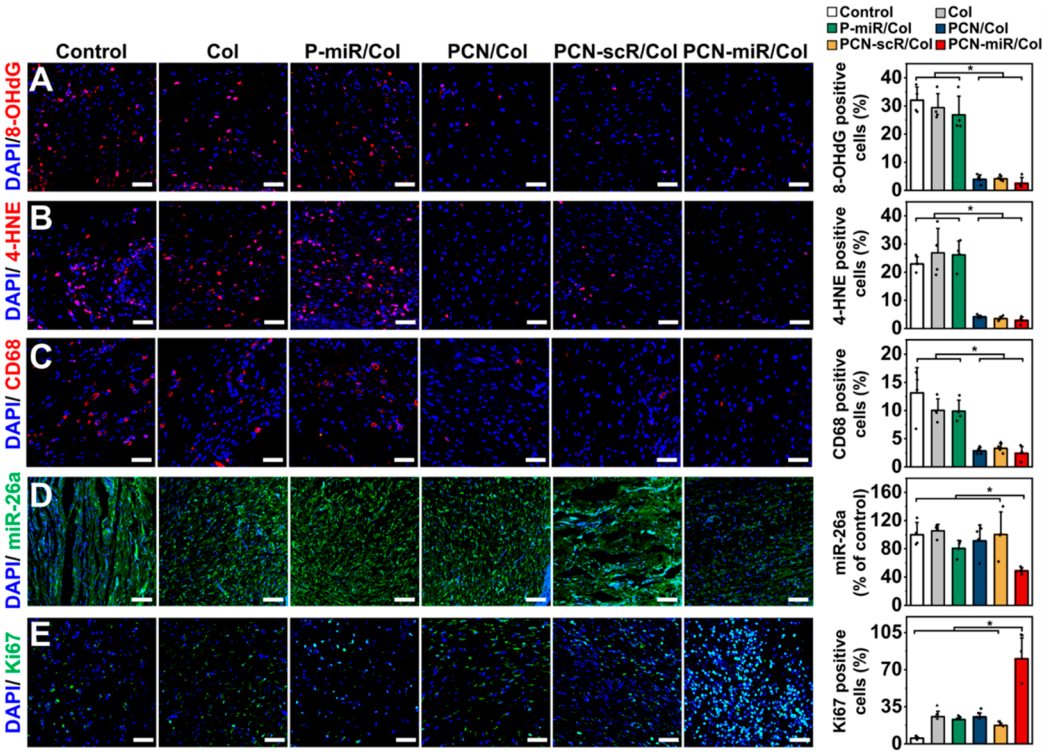

Figure 4. *In vivo* topical application of PCN-miR/Col reshapes the highly oxidative and inflammatory wound microenvironment and corrects miR-26a overexpression. Representative confocal images of immunofluorescence staining and quantification for (A) 8-OHdG (a marker of oxidative DNA damage), (B) 4-HNE (a marker of lipid peroxidation), (C) CD68-positive macrophages, (D) miR-26a, and (E) Ki67-positive cells in sections from each group after 28 days of treatment (n = 4). Scale bars for 8-OHdG, 4-HNE, CD68, and Ki67 images, 50 μm; Scale bars for miR-26a image, 100 μm. All results are presented as mean ± SD, *P < 0.05 by two-tailed unpaired Student's t tests.

notably in miR/Col and P-miR/Col after ROS exposure, indicating that the N-C═O bonds in the collagen matrix cleave upon oxidative damage (Figure 2H). Furthermore, although a small new peak corresponding to the O-C═O bond was also observed, C1s XPS spectra of PCN-miR/Col did not change significantly before and after ROS exposure, which confirms the lack of a drastic denaturing process (Figure 2H). Circular dichroism (CD) spectra were obtained before and after ROS exposure, which are highly sensitive to three-dimensional conformations of proteins.[35] Before ROS exposure, the collagen hydrogels showed a similar triple-helical CD signal pattern with a positive peak at 220-221 nm and a negative peak at 197-198 nm, suggesting that the incorporation of antagomiR-26a and ceria nanozymes had a negligible influence on the secondary structures of collagen proteins (Figure 2I). Subjecting the miR/Col and P-miR/Col hydrogels to ROS resulted in a sharp decrease in negative ellipticity (Figure 2I). By contrast, PCN-miR/Col exhibited only a minimal decrease in the negative CD signal after ROS exposure, confirming greater stability of the helical structure in the collagen matrix (Figure 2I). Collectively, these results support the concept that incorporation of ceria nanozymes endows the collagen hydrogel with resistance to oxidative damage, which can greatly enhance the efficacy of the fragile antagomiR-26a for diabetic wound healing in the highly oxidative wound bed.

PCN-miR/Col Protects Cells against Harmful Oxidative Damage. The biocompatibility is a prerequisite for biomedical applications. As shown in Figure S3A,B, PCNs and PCN-miR had no obvious cytotoxicity compared with PEI_{25k} and PEI_{25k} (P) antagomiR-26a (miR) complex (P-miR), indicating that functionalization of PEI_{25k} with ceria nanozymes did not result in additional toxicity. In addition, the cytotoxicity of PCN was lower than that of PEI_{25k}, indicating that the increased generation of ROS by PEI_{25k} can be scavenged by the ceria nanozyme.[36] We further explored the cell uptake behaviors by confocal laser scanning microscopy (CLSM) using a fluorescently (Cy5) labeled antagomiR-26a. The human umbilical vein endothelial cells (HUVECs) exhibited a much stronger fluorescence signal of antagomiR-26a after incubation with PCN-miR compared to that generated after incubation with P-miR complexes or naked antagomiR-26a (Figure S3C). Since both PCN-miR and P-miR contain PEI_{25K} polycations, this discrepancy in cellular uptake arises from the ceria nanozymes, which is consistent with many previous reports using inorganic nanoparticles as carriers for nucleic acids.[37] Furthermore, the CLSM images clearly revealed no obvious change in cell viability after 4 days of incubation with the PCN-miR/Col hydrogel, indicating that the PCN-miR/Col hydrogel is highly biocompatible (Figure S3D). We next evaluated whether this redox-active nanocomposite hydrogel could protect cells and intracellular biomacromolecules against harmful oxidative damage. HUVECs were preincubated with the hydrogels and then challenged with H_2O_2 to simulate an oxidative microenvironment. HUVECs preincubated with miR/Col or P-miR/Col exhibited significant cell mortality upon oxidative stress, whereas the PCN-miR/Col group showed only minimal reduction in cell viability (Figure 3A). The ceria nanozymes incorporating PCN-miR/Col significantly boosted the extent of ROS-scavenging, with the greatest reduction in mean cell fluorescence of the ROS probe 2′-7′-dichorofluorescein

DOI: 10.1021/acscentsci.8b00850
ACS Cent. Sci. 2019, 5, 477−485

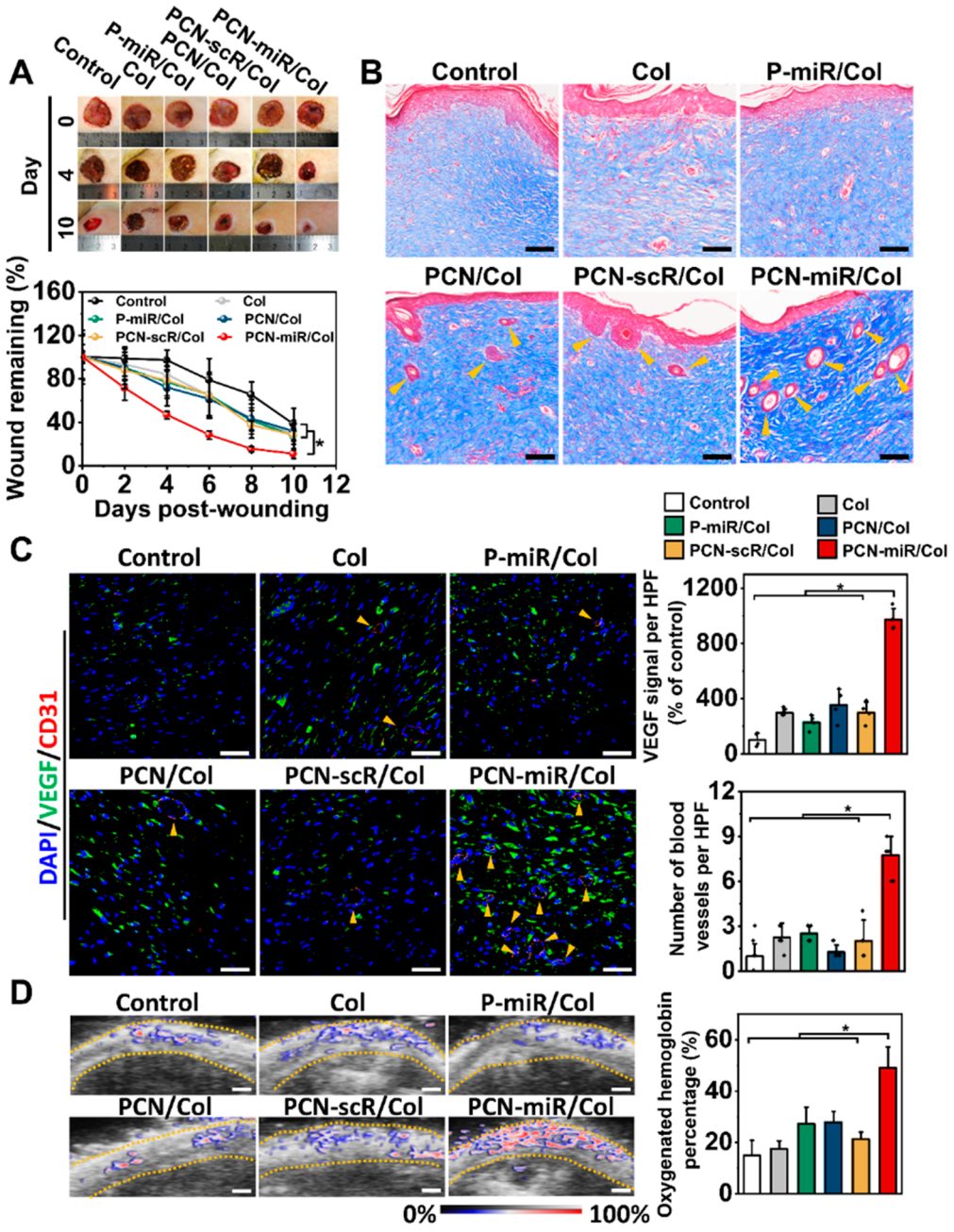

Figure 5. PCN-miR/Col induces accelerated and regenerative diabetic wound healing *in vivo*. (A) Digital images of wounds at day 0, 4, and 10 after the indicated treatment (left panel) and quantification of wound closure as a percentage of the initial wound area (right panel, $n = 5$). (B) Masson's trichrome staining of representative wound tissues from each group after 28 days of treatment. Scale bars, 100 μm. (C) Representative confocal images of VEGF and CD31 double-stained sections and quantification for VEGF expression and number of blood vessels per high-powered field (HPF) from each group at day 28. Scale bars, 50 μm. $n = 4$. (D) Photoacoustic images and quantification for oxygenated hemoglobin from each group at day 28. Scale bars, 1 mm. $n = 3$. All results are presented as mean ± SD, $^*P < 0.05$ by two-tailed unpaired Student's t tests.

(DCF) (Figure S4A). These results were further confirmed by CLSM observations (Figure 3B, Figure S4B).

Subcellular components are highly susceptible to ROS-induced oxidative damage, resulting in their functional impairment. We next examined the impact of PCN-miR/Col on the responses of subcellular components to toxic ROS. After H_2O_2 exposure, cells pretreated with miR/Col or P-miR/Col displayed reduced mitochondrial polarization (as determined by the 5,5′,6,6′-tetrachloro-1,1′,3,3′-tetraethylimidacarbocyanine (JC-1) aggregate:monomer ratio) compared to cells pretreated with PCN-miR/Col (Figure 3C, Figure S4C). The level of double-stranded DNA damage was determined with immunofluorescence of phosphorylated H2A histone family member X (γ-H2AX). Compared to miR/Col or P-miR/Col pretreatment, cells pretreated with PCN-miR/Col showed significantly diminished accumulation of DNA damage foci after oxidative insult (Figure 3D, Figure S4D). Similar differential behaviors in the contents of the lipid peroxidation product malondialdehyde (MDA) and carbonylated proteins were also detected among the groups upon H_2O_2 exposure, thus further supporting that PCN-miR/Col could attenuate the oxidative damage of these subcellular

DOI: 10.1021/acscentsci.8b00850
ACS Cent. Sci. 2019, 5, 477−485

components (Figure 3E,F). Collectively, these data demonstrated that the ROS-modulating hydrogel PCN-miR/Col confers robust cellular protection against ROS accumulation (Figure 3G). Previous studies have shown that cells exposed to the oxidative microenvironment exhibited enhanced cellular senescence, leading to the impairment for functional angiogenesis and tissue regeneration.[38] Indeed, because of their limited capabilities in ROS-scavenging, the miR/Col- or P-miR/Col-pretreated cells challenged with H_2O_2 acquired a significant senescent phenotype with high levels of senescence-associated β-galactosidase (SA-β-gal) activity in comparison to those pretreated with PCN-miR/Col (Figure S4E).

PCN-miR/Col Reshapes the Wound Microenvironment and Corrects miR-26a Overexpression. We next explored the therapeutic effect of these collagen-based hydrogels in a streptozotocin-induced (STZ-induced) diabetic wound rat model. Diabetic excisional wounds were created in STZ-induced diabetic rats, which were topically treated with a series of collagen hydrogels: (i) collagen hydrogel alone (Col), (ii) P-miR/Col, (iii) PCN-loaded collagen hydrogel (PCN/Col), (iv) PCN-scrambled miRNA (scR) nanocomplex (PCN-scR) loaded collagen hydrogel (PCN-scR/Col), and (v) PCN-miR/Col. Immunofluorescence staining of wound tissues displayed increased amounts of oxidative DNA damage marker 8-hydroxydeoxyguanosine (8-OHdG) after treatments with the hydrogels without containing ceria nanozymes (Col and P-miR/Col) and the blank control, whereas much lower 8-OHdG levels were detected in the wounds of diabetic rats treated with hydrogels loaded with the ceria nanozymes (PCN/Col, PCN-scR/Col, and PCN-miR/Col) (Figure 4A). Similar differential results in the contents of the lipid peroxidation marker 4-hydroxy-2-nonenal (4-HNE) were also observed (Figure 4B). Notably, the skin tissues from diabetic rats, but not from healthy rats, presented robust oxidative damage signals (8-OHdG and 4-HNE) and insufficient proliferation markers Ki67 (Figure S5).

Studies have revealed that continued oxidative stress can lead to unresolved inflammation.[1] As an efficient antioxidant agent, ceria nanozyme demonstrated excellent anti-inflammation effect.[39] Robust infiltration of CD68-positive monocytes/macrophages was clearly observed in wound tissues treated with hydrogels without containing ceria nanozymes (Col and P-miR/Col) and the blank control, while substantially milder infiltration of monocytes/macrophages was detected in the wounds treated with ceria nanozyme-loaded hydrogels (PCN/Col, PCN-scR/Col, and PCN-miR/Col) (Figure 4C). Wounds treated with PCN-miR/Col displayed only a modest miR-26a signal, while intensive fluorescence of miR-26a was detected in wound tissues treated with the other groups (Figure 4D). The failure of P-miR/Col to inhibit miR-26a can be attributed to the lack of protection for antagomiR-26a against the highly oxidative microenvironment. Furthermore, wounds treated with PCN-miR/Col had a markedly higher frequency of the proliferation marker Ki67-expressing cells in comparison to those of the other groups (Figure 4E). Collectively, these findings suggested that the PCN-miR/Col hydrogel was endowed with the capacity to reshape the highly oxidative wound microenvironment and miR-26a overexpression.

PCN-miR/Col Induces Accelerated and Regenerative Diabetic Wound Healing. The PCN-miR/Col treatment group displayed significantly faster wound closure than that of the other five groups (Figure 5A). Wounds treated with PCN-miR/Col exhibited a smooth yellowish appearance, like healthy skin, whereas wounds treated with other groups displayed an ulcerative reddish surface (Figure S6). Staining of wound sections with Masson's trichrome revealed a significant increase in collagen fiber density and marked regeneration of skin appendages in the PCN-miR/Col-treated wounds (Figure 5B). SEM imaging demonstrated a highly ordered alignment of collagen fiber in the PCN-miR/Col-treated wounds, whereas the collagen fibers from the wounds of control groups were more disarranged and tangled (Figure S7). Picrosirius red staining further confirmed increased collagen deposition in PCN-miR/Col-treated wounds with a predominantly yellow–orange (collagen I) appearance in comparison to wounds treated with other groups, which mainly showed smaller green collagen fibers (collagen type III) (Figure S8). Remarkably, the intact diabetic skin and nondiabetic skin also displayed a highly ordered collagen fiber alignment with predominant yellow–orange staining (collagen type I) (Figure S9A). The type I/III collagen ratio in the PCN-miR/Col-treated wounds was significantly increased compared with those of other groups (Figure S9B). The relatively high type I/III collagen ratio indicates successful collagen maturation and enhanced mechanical strength of the healed wound tissue, which would make the wound more resistant to reinjury.[40] In addition, H&E staining demonstrated no significant toxicity in the major organs of the treated rats (Figure S10).[41]

As shown in Figure 5C, diabetic wounds treated with PCN-miR/Col displayed pronounced VEGF expression and blood vessel formation in comparison to those of the other groups. The function of these newly formed blood vessels was further examined using a high-frequency ultrasound and photoacoustic microimaging system. Interestingly, a significantly higher proportion of oxygenated hemoglobin was observed in the wound tissues treated with PCN-miR/Col compared to the other treatments, suggesting that PCN-miR/Col resulted in marked improvement in the oxygen supply (Figure 5D). Collectively, these data indicated that structural and functional blood vessels were successfully re-established in PCN-miR/Col-treated diabetic wounds.

CONCLUSIONS

In summary, we adopted the "seed-and-soil" concept in the regenerative medicine field to guide the design of biomaterials for addressing the underlying pathological mechanisms of impaired diabetic wound healing.[2,6] To simultaneously provide a proregenerative wound microenvironment (the "soil") and proangiogenic cues (the "seed") for diabetic wound repair and regeneration, we developed PCN-miR/Col, an antagomiR-26a-impregnated redox-active self-protecting hydrogel. As a proof of concept, we demonstrate that the PCN-miR/Col can protect the incorporated proangiogenic antagomiR-26a from denaturation by ROS exposure and efficiently alleviate oxidative damage both *in vitro* and *in vivo*. Immunofluorescence and photoacoustic imaging analyses further reveal that PCN-miR/Col markedly promotes the vascular regeneration and oxygen supply in the wound bed. As a result, the PCN-miR/Col treatment yielded significantly improved diabetic wound repair and regeneration with an accelerated wound healing rate, marked regeneration of skin appendages, and enhanced collagen deposition in the wound bed. To the best of our knowledge, our study represents the first demonstration of a multifunctional hydrogel, which offers both the proregenerative wound microenvironment (the microenvironmental cues, "soil") and proangiogenic miRNAs (the biochemical cues,

DOI: 10.1021/acscentsci.8b00850
ACS Cent. Sci. 2019, 5, 477−485

"seed") for functional angiogenesis and regenerative diabetic wound healing.

■ ASSOCIATED CONTENT

Supporting Information

The Supporting Information is available free of charge on the ACS Publications website at DOI: 10.1021/acscentsci.8b00850.

Additional experimental methods and figures including size distribution, TEM, SEM, AFM characterization of ceria nanozymes, PCN-miR and collagen-based hydrogels, biocompatibility and cellular uptake evaluation, assessment of *in vitro* ROS-scavenging capacity, immunofluorescence staining for 8-OHdG and 4-HNE, ultrastructure of collagen fibers, and systemic toxicity evaluation (PDF)

■ AUTHOR INFORMATION

Corresponding Authors

*E-mail: gaojianqing@zju.edu.cn.
*E-mail: lingds@zju.edu.cn.

ORCID

Haibin Wu: 0000-0002-9043-0869
Jianqing Gao: 0000-0003-1052-7060
Daishun Ling: 0000-0002-9977-0237

Author Contributions

⊥H.W. and F.L. contributed equally.

Notes

The authors declare no competing financial interest.
Safety statement: no unexpected or unusually high safety hazards were encountered.

■ ACKNOWLEDGMENTS

We gratefully acknowledge the support from the National Key Research and Development Program of China (2016YFA0203600), the National Natural Science Foundation of China (31822019, 51703195, 91859116, 81620108028), One Belt and One Road International Cooperation Project from Key Research and Development Program of Zhejiang Province (2019C04024), the Zhejiang Provincial Natural Science Foundation of China(LGF19C100002), "Thousand Talents Program" for Distinguished Young Scholars, Fundamental Research Funds for the Central Universities (2018QNA7020), and Zhejiang Provincial Program for the Cultivation of High-Level Innovative Health Talents.

■ REFERENCES

(1) Falanga, V. Wound healing and its impairment in the diabetic foot. *Lancet* **2005**, *366*, 1736−1743.
(2) Armstrong, D. G.; Boulton, A. J. M.; Bus, S. A. Diabetic foot ulcers and their recurrence. *N. Engl. J. Med.* **2017**, *376*, 2367−2375.
(3) Marino, D.; Luginbuhl, J.; Scola, S.; Meuli, M.; Reichmann, E. Bioengineering dermo-epidermal skin grafts with blood and lymphatic capillaries. *Sci. Transl. Med.* **2014**, *6*, 221ra14.
(4) Wang, H.; Agarwal, P.; Xiao, Y.; Peng, H.; Zhao, S.; Liu, X.; Zhou, S.; Li, J.; Liu, Z.; He, X. A nano-in-micro system for enhanced stem cell therapy of ischemic diseases. *ACS Cent. Sci.* **2017**, *3*, 875−885.
(5) Duscher, D.; Neofytou, E.; Wong, V. W.; Maan, Z. N.; Rennert, R. C.; Inayathullah, M.; Januszyk, M.; Rodrigues, M.; Malkovskiy, A. V.; Whitmore, A. J.; et al. Transdermal deferoxamine prevents pressure-induced diabetic ulcers. *Proc. Natl. Acad. Sci. U. S. A.* **2015**, *112*, 94−99.
(6) Forbes, S. J.; Rosenthal, N. Preparing the ground for tissue regeneration: from mechanism to therapy. *Nat. Med.* **2014**, *20*, 857−869.
(7) Nakada, Y.; Canseco, D. C.; Thet, S.; Abdisalaam, S.; Asaithamby, A.; Santos, C. X.; Shah, A. M.; Zhang, H.; Faber, J. E.; Kinter, M. T.; et al. Hypoxia induces heart regeneration in adult mice. *Nature* **2017**, *541*, 222−227.
(8) Speidel, A. T.; Stuckey, D. J.; Chow, L. W.; Jackson, L. H.; Noseda, M.; Abreu Paiva, M.; Schneider, M. D.; Stevens, M. M. Multimodal hydrogel-based platform to deliver and monitor cardiac progenitor/stem cell engraftment. *ACS Cent. Sci.* **2017**, *3*, 338−348.
(9) Park, S.-j.; Park, W.; Na, K. Tumor intracellular-environment responsive materials shielded nano-complexes for highly efficient light-triggered gene delivery without cargo gene damage. *Adv. Funct. Mater.* **2015**, *25*, 3472−3482.
(10) Warren, C. M.; Ziyad, S.; Briot, A.; Der, A.; Iruela-Arispe, M. L. A ligand-independent VEGFR2 signaling pathway limits angiogenic responses in diabetes. *Sci. Signal.* **2014**, *7*, ra1.
(11) Benndorf, R. A.; Schwedhelm, E.; Gnann, A.; Taheri, R.; Kom, G.; Didie, M.; Steenpass, A.; Ergun, S.; Boger, R. H. Isoprostanes inhibit vascular endothelial growth factor-induced endothelial cell migration, tube formation, and cardiac vessel sprouting in vitro, as well as angiogenesis in vivo via activation of the thromboxane A(2)receptor: a potential link between oxidative stress and impaired angiogenesis. *Circ. Res.* **2008**, *103*, 1037−1046.
(12) Schaper, N. C.; Van Netten, J. J.; Apelqvist, J.; Lipsky, B. A.; Bakker, K. Prevention and management of foot problems in diabetes: a summary guidance for daily practice 2015, based on the IWGDF guidance documents. *Diabetes/Metab. Res. Rev.* **2016**, *32*, 7−15.
(13) Sunkari, V. G.; Lind, F.; Botusan, I. R.; Kashif, A.; Liu, Z.-J.; Ylä-Herttuala, S.; Brismar, K.; Velazquez, O.; Catrina, S.-B. Hyperbaric oxygen therapy activates hypoxia-inducible factor 1 (HIF-1), which contributes to improved wound healing in diabetic mice. *Wound Repair Regen* **2015**, *23*, 98−103.
(14) Mirabella, T.; MacArthur, J. W.; Cheng, D.; Ozaki, C. K.; Woo, Y. J.; Yang, M.; Chen, C. S. 3D-printed vascular networks direct therapeutic angiogenesis in ischaemia. *Nat. Biomed. Eng.* **2017**, *1*, 83.
(15) Briquez, P. S.; Clegg, L. E.; Martino, M. M.; Mac Gabhann, F.; Hubbell, J. A. Design principles for therapeutic angiogenic materials. *Nat. Rev. Mater.* **2016**, *1*, 1−15.
(16) Li, S.; Nih, L. R.; Bachman, H.; Fei, P.; Li, Y.; Nam, E.; Dimatteo, R.; Carmichael, S. T.; Barker, T. H.; Segura, T. Hydrogels with precisely controlled integrin activation dictate vascular patterning and permeability. *Nat. Mater.* **2017**, *16*, 953−961.
(17) Zhang, Q.; Chen, F.; Xu, F.; Zhao, Y.; Fan, C. Target-triggered three-way junction structure and polymerase/nicking enzyme synergetic isothermal quadratic DNA machine for highly specific, one-step, and rapid microRNA detection at attomolar level. *Anal. Chem.* **2014**, *86*, 8098−8105.
(18) Icli, B.; Nabzdyk, C. S.; Lujan-Hernandez, J.; Cahill, M.; Auster, M. E.; Wara, A. K. M.; Sun, X.; Ozdemir, D.; Giatsidis, G.; Orgill, D. P.; et al. Regulation of impaired angiogenesis in diabetic dermal wound healing by microRNA-26a. *J. Mol. Cell. Cardiol.* **2016**, *91*, 151−159.
(19) Kota, J.; Chivukula, R. R.; O'Donnell, K. A.; Wentzel, E. A.; Montgomery, C. L.; Hwang, H.-W.; Chang, T.-C.; Vivekanandan, P.; Torbenson, M.; Clark, K. R.; et al. Therapeutic microRNA delivery suppresses tumorigenesis in a murine liver cancer model. *Cell* **2009**, *137*, 1005−1017.
(20) Brown, B. D.; Naldini, L. Exploiting and antagonizing microRNA regulation for therapeutic and experimental applications. *Nat. Rev. Genet.* **2009**, *10*, 578−585.
(21) Halliwell, B. Reactive oxygen species in living systems: Source, biochemistry, and role in human disease. *Am. J. Med.* **1991**, *91*, S14−S22.
(22) Hamdan, S.; Pastar, I.; Drakulich, S.; Dikici, E.; Tomic-Canic, M.; Deo, S.; Daunert, S. Nanotechnology-driven therapeutic

DOI: 10.1021/acscentsci.8b00850
ACS Cent. Sci. 2019, 5, 477−485

interventions in wound healing: Potential uses and applications. *ACS Cent. Sci.* **2017**, *3*, 163−175.
(23) Kim, C. K.; Kim, T.; Choi, I. Y.; Soh, M.; Kim, D.; Kim, Y. J.; Jang, H.; Yang, H. S.; Kim, J. Y.; Park, H. K. Ceria nanoparticles that can protect against ischemic stroke. *Angew. Chem., Int. Ed.* **2012**, *51*, 11039−11043.
(24) You, L.; Wang, J.; Liu, T.; Zhang, Y.; Han, X.; Wang, T.; Guo, S.; Dong, T.; Xu, J.; Anderson, G. J.; et al. Targeted brain delivery of rabies virus glycoprotein 29-modified deferoxamine-loaded nanoparticles reverses functional deficits in parkinsonian mice. *ACS Nano* **2018**, *12*, 4123−4139.
(25) Xu, C.; Qu, X. Cerium oxide nanoparticle: a remarkably versatile rare earth nanomaterial for biological applications. *NPG Asia Mater.* **2014**, *6*, No. e90.
(26) Chao, Y.; Xu, L.; Liang, C.; Feng, L.; Xu, J.; Dong, Z.; Tian, L.; Yi, X.; Yang, K.; Liu, Z. Combined local immunostimulatory radioisotope therapy and systemic immune checkpoint blockade imparts potent antitumour responses. *Nat. Biomed. Eng.* **2018**, *2*, 611−621.
(27) Whyte, W.; Roche, E. T.; Varela, C. E.; Mendez, K.; Islam, S.; O'Neill, H.; Weafer, F.; Shirazi, R. N.; Weaver, J. C.; Vasilyev, N. V.; et al. Sustained release of targeted cardiac therapy with a replenishable implanted epicardial reservoir. *Nat. Biomed. Eng.* **2018**, *2*, 416−428.
(28) Zhang, X.; Zhou, H.; Xie, Y.; Ren, C.; Ding, D.; Long, J.; Yang, Z. Rational design of multifunctional hetero-hexameric proteins for hydrogel formation and controlled delivery of bioactive molecules. *Adv. Healthcare Mater.* **2014**, *3*, 1804−1811.
(29) Wang, M.; Liu, H.; Li, L.; Cheng, Y. A fluorinated dendrimer achieves excellent gene transfection efficacy at extremely low nitrogen to phosphorus ratios. *Nat. Commun.* **2014**, *5*, 3053.
(30) Macaya, D.; Ng, K. K.; Spector, M. Injectable collagen-genipin gel for the treatment of spinal cord injury: in vitro studies. *Adv. Funct. Mater.* **2011**, *21*, 4788−4797.
(31) Singh, D. K.; Winocour, P.; Farrington, K. Oxidative stress in early diabetic nephropathy: fueling the fire. *Nat. Rev. Endocrinol.* **2011**, *7*, 176−184.
(32) Lin, L.-S.; Song, J.; Song, L.; Ke, K.; Liu, Y.; Zhou, Z.; Shen, Z.; Li, J.; Yang, Z.; Tang, W.; et al. Simultaneous fenton-like ion delivery and glutathione depletion by MnO_2-based nanoagent to enhance chemodynamic therapy. *Angew. Chem.* **2018**, *130*, 4996−5000.
(33) Dutta, A.; Gautam, R.; Chatterjee, S.; Ariese, F.; Sikdar, S. K.; Umapathy, S. Ascorbate protects neurons against oxidative stress: A raman microspectroscopic study. *ACS Chem. Neurosci.* **2015**, *6*, 1794−1801.
(34) Chiang, S.-C.; Meagher, M.; Kassouf, N.; Hafezparast, M.; McKinnon, P. J.; Haywood, R.; El-Khamisy, S. F. Mitochondrial protein-linked DNA breaks perturb mitochondrial gene transcription and trigger free radical-induced DNA damage. *Sci. Adv.* **2017**, *3*, e1602506−e1602516.
(35) Greenfield, N. J. Using circular dichroism spectra to estimate protein secondary structure. *Nat. Protoc.* **2007**, *1*, 2876−2890.
(36) Kuo, J.-h. S.; Jan, M.-s.; Lin, Y.-L. Interactions between U-937 human macrophages and poly(propyleneimine) dendrimers. *J. Controlled Release* **2007**, *120*, 51−59.
(37) Sokolova, V.; Epple, M. Inorganic ncanoparticles as carriers of nucleic acids into cells. *Angew. Chem., Int. Ed.* **2008**, *47*, 1382−1395.
(38) Jeon, O. H.; Kim, C.; Laberge, R. M.; Demaria, M.; Rathod, S.; Vasserot, A. P.; Chung, J. W.; Kim, D. H.; Poon, Y.; David, N.; et al. Local clearance of senescent cells attenuates the development of post-traumatic osteoarthritis and creates a pro-regenerative environment. *Nat. Med.* **2017**, *23*, 775−781.
(39) Hirst, S. M.; Karakoti, A. S.; Tyler, R. D.; Sriranganathan, N.; Seal, S.; Reilly, C. M. Anti-inflammatory properties of cerium oxide nanoparticles. *Small* **2009**, *5*, 2848−2856.
(40) Wang, T.; Gu, Q.; Zhao, J.; Mei, J.; Shao, M.; Pan, Y.; Zhang, J.; Wu, H.; Zhang, Z.; Liu, F. Calcium alginate enhances wound healing by up-regulating the ratio of collagen types I/III in diabetic rats. *Int. J. Clin. Exp. Pathol.* **2015**, *8*, 6636−6645.
(41) Feliu, N.; Docter, D.; Heine, M.; del Pino, P.; Ashraf, S.; Kolosnjaj-Tabi, J.; Macchiarini, P.; Nielsen, P.; Alloyeau, D.; Gazeau, F.; et al. In vivo degeneration and the fate of inorganic nanoparticles. *Chem. Soc. Rev.* **2016**, *45*, 2440−2457.

DOI: 10.1021/acscentsci.8b00850
ACS Cent. Sci. 2019, 5, 477−485